Quantum size effects in the atomistic structure of armchair nanoribbons

A. Dasgupta,[1] S. Bera,[1,2,3,*] F. Evers,[1,2,3] and M. J. van Setten[1,3,†]

[1]*Institute of Nanotechnology, Karlsruhe Institute of Technology, D-76021 Karlsruhe, Germany*

[2]*Institut für Theorie der Kondensierten Materie, Karlsruhe Institute of Technology, D-76128 Karlsruhe, Germany*

[3]*DFG Center for Functional Nanostructures, Karlsruhe Institute of Technology, D-76131 Karlsruhe, Germany*

(Received 11 November 2011; revised manuscript received 1 February 2012; published 26 March 2012)

Quantum size effects in armchair graphene nanoribbons (AGNRs) with hydrogen termination are investigated via density functional theory (DFT) in the Kohn-Sham formulation. "Selection rules" are formulated, which allow extraction (approximately) the electronic structure of the AGNR bands starting from the four graphene dispersion sheets. In analogy with the case of carbon nanotubes, a threefold periodicity of the excitation gap with the ribbon width (N; number of carbon atoms per carbon slice) is predicted, which is confirmed by *ab initio* results. While traditionally such a periodicity would be observed in electronic response experiments, the DFT analysis presented here shows that it can also be seen in the ribbon geometry: the length of a ribbon with L slices approaches the limiting value for a very large width, $1 \ll N$ (keeping the aspect ratio low, $N \ll L$), with $1/N$ oscillations that display electronic selection rules. The oscillation amplitude is so strong that the asymptotic behavior is nonmonotonous, i.e.; wider ribbons exhibit a stronger elongation than narrower ones.

DOI: 10.1103/PhysRevB.85.125433 PACS number(s): 73.21.Hb, 61.48.De, 73.22.Pr

I. INTRODUCTION

Its nonstandard electronic properties[1,2] along with improved fabrication techniques have moved graphene and its allotropes into the focus of frontier research in recent times.[3] The presence of an edge in graphene nanoribbons (GNRs) has a significant influence on these electronic structures.[4–7] In contrast to pure graphene, GNRs with a proper edge exhibit a finite bandgap potentially useful for device applications. Therefore, graphene nanostructures with a well-defined orientation and edges have become a research field of their own.[7–19]

As is well known, zigzag-edged ribbons have two flat metallic bands near the Fermi energy, possibly leading to magnetism.[20–22] By contrast, armchair GNRs (AGNRs) are semiconducting, with width-dependent bandgaps and without an affinity for magnetic instabilities.[4,23–31] In this paper we further investigate the electronic and atomistic structure of monohydrogenated AGNRs and show that interesting quantum effects arise, nevertheless. We formulate selection rules for the transverse momenta of the ribbon. They identify those lines in the (extended) Brillouin zone of graphene that resemble the electronic structure of AGNRs of a given width N, the number of carbon atoms in the transverse direction (see Fig. 1). In this way we infer that a reasonable first approximation for all energy bands of an AGNR is encoded in a single selection rule. Similarly to the case of a carbon nanotube (CNT), the selection rule predicts a threefold periodicity of the bandgap in N. Because the same selection rule can be applied to all bands, one might expect this periodicity to appear also in the atomic structure of the ribbon. Indeed, this is what has been observed previously for the edge stress and energy of nonpassivated ribbons.[32] Our detailed density functional theory (DFT) anatomy of AGNRs reveals, however, that the threefold periodicity also appears in the atomic structure of hydrogen-terminated AGNRs: the longitudinal deformation of the unit cell of an AGNR with respect to the bulk graphene value is described in leading harmonic approximation by the term $\sim\cos(2\pi N/3)/(N-1)$.

Our results imply that quantum size effects can be studied experimentally in AGNRs by atomic structure determination, namely, by comparing the length of AGNRs (having the same number of carbon slices, L) of neighboring width $N, N+1, \ldots$. This is in marked contrast to traditional approaches in meso- and nanoscopic structures that investigate quantum size effects near the bandgap by directly probing the electronic excitation spectrum, e.g., in transport measurements.

II. METHOD AND MODEL

All DFT calculations presented in this paper are performed using a plane-wave basis set and the projector-augmented wave (PAW) method,[33,34] as implemented in the Vienna *Ab initio* Simulation Package (VASP).[35–37] The choice of the exchange correlation functional was made on the basis of a comparison of lattice parameters for bulk graphene obtained with different functionals (see Table I). The comparison shows only little variation. The results using the generalized gradient approximations (GGAs) are in general closer to the experimental value than those using the local density approximation (LDA).[40] The results for the LDA and GGA found here are in agreement with previous calculations (see, e.g., Ref. 19 and references therein). Based on these results the exchange-correlation functional of Perdew and Wang was chosen.[38]

For all geometries, the atomic structure is fully optimized using a conjugate gradient algorithm. A convergency criterion of 1 meV/Å is used for the forces on the atoms. All supercells used contain a vacuum layer in the direction perpendicular to the layers (z direction) of 24 Å. The unit cells of the ribbons additionally contain a vacuum layer of ∼17 Å between the ribbons in the plane of the ribbons (y direction), thereby retaining periodicity in the x direction only. These vacuum layers diminish all interactions between periodic images to a degree that the total energies are converged within 1 meV. The reciprocal space is sampled by $24 \times 24 \times 1$ for the bulk and by $200 \times 1 \times 1$ for the ribbons, giving total energies again

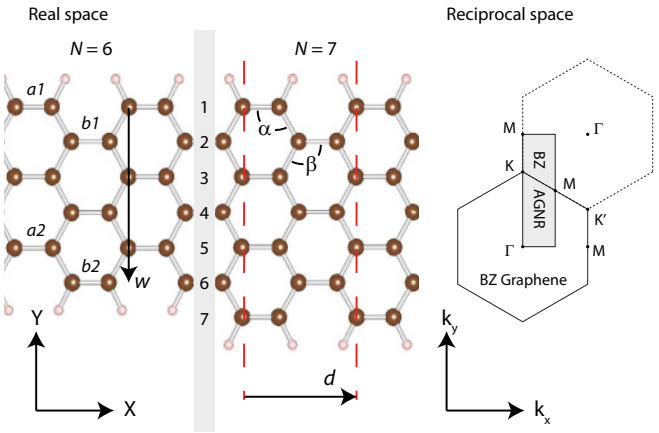

FIG. 1. (Color online) Left: Atomistic structure of armchair graphene nanoribbons (AGNRs). They come in two species, with odd and even numbers of carbon atoms N in the transverse direction. Right: Brillouin zone of graphene appropriately parameterized for locating energy bands in the AGNR.

converged well within 1 meV. A Gaussian smearing with a width of 0.05 eV and a kinetic energy cutoff of 700 eV for the plane-wave basis set is used in all cases.

III. ELECTRONIC STRUCTURE OF AN H-TERMINATED AGNR

In Fig. 2 the gap for electronic excitations of an AGNR is plotted over the inverse system width. The data split into three sets exhibiting an oscillatory behavior.[30] For $N+1$ divisible by 3, the smallest gaps $\Delta(N)$ are seen and interpolate smoothly with $1/N$ into the bulk limit $\Delta = 0$. For N divisible by 3, the gaps are larger, also interpolating smoothly into $\Delta = 0$. The largest gaps are encountered in the remaining case, $N-1$ divisible by 3.

This overall phenomenology is reminiscent of the situation with CNTs,[41] and we investigate it closely now. Zigzag CNTs are similar to AGNRs with the H termination replaced by periodic boundary conditions. The tube's electronic structure is understood by imposing selection rules for allowed transverse wave numbers on graphene's band structure in reciprocal **k** space. These selection rules reflect the cylindrical geometry. Three classes of armchair CNTs are thus obtained.[41] In a very similar way, the electronic structure of an AGNR can also be

TABLE I. Lattice parameter, expressed as a (Å), d (Å), and C–C (Å) and elasticity, and $\lambda+\mu$ (eV Å^{-2}) of bulk graphene calculated using the LDA, GGA-PW91, GGA-PBE, and meta-GGA (PBE-PKZB) approximations to the exchange correlation functional (XC) compared to experimental values.[38,39]

XC	a	d	C–C	$\lambda+\mu$
LDA	2.447	4.2387	1.4129	8.87
GGA-PW91	2.466	4.2718	1.4239	9.11
GGA-PBE	2.468	4.274	1.425	9.10
Meta-GGA	2.480	4.2955	1.4318	9.01
Expt. (graphite)	2.4612	4.2629	1.4210	

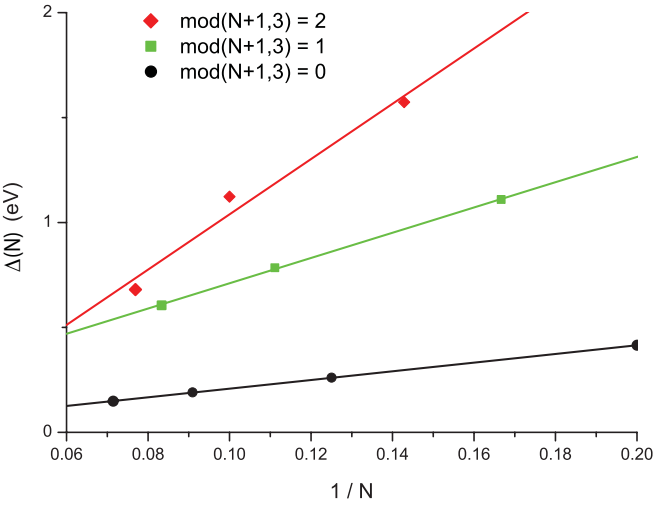

FIG. 2. (Color online) Bandgap $\Delta(N)$ of hydrogen-terminated AGNRs as a function of $1/N$.

understood as a cut through graphene's dispersion sheets along lines of selected transverse momenta k_y.[42]

To find the appropriate selection rule for AGNRs we map the (valence) bands $\epsilon(k_x)$ of the $N = 5$–9 ribbons onto the four (valence) dispersion sheets, $\epsilon(k_x,k_y)$, of pure graphene. The sheets are plotted as color maps in Fig. 3. For each sheet, k_y values in graphene's Brillouin zone were selected such that the set of $\epsilon_{k_y}(k_x)$ functions obtained most closely resembles the band structure of the AGNR. (Comparison of the functions for fitted k_y to the actual ribbons bands is shown for all four sheets of the $N = 5$ to $N = 9$ AGNRs in Figs. 7 to 11 in the Appendix.) The fitting process produces N bands in sheets 1, 2, and 4. Due to the H atoms at the edges, the third sheet accommodates two more bands, $N+2$.

We infer from Fig. 3 that in sheets 1, 2, and 4 the AGNR bands are approximately equidistant, with $\Delta k_y \approx k_{\max}/(N+1)$, which motivates the selection rule,

$$\{k_y\} = \bigcup_i \frac{i}{N+1} k_{\max}, \quad k_{\max} = \frac{4\pi}{\sqrt{3}a_0}, \tag{1}$$

where i runs from 1 to N for the sheets 1, 2, and 4 and from 0 to $N+1$ for sheet 3, to also include the two H bands.

AGNR bands as predicted by the rules, Eq. (1), are also indicated in Fig. 3; the root mean square deviations per sheet of the fitted values to the selection rule predictions are detailed ing Fig. 4. We find a good match for the uppermost sheet 4, especially in the vicinity of the K point. The overall discrepancy between the predicted and the true transverse momenta of the ribbon bands never exceeds 15% of the interband spacing. An exception to this rule is presented by the third sheet. Here, the presence of H atoms interferes and the selection rule gives only semiquantitative information.

In analogy to the case of CNTs, the proposed rules, (1), also allow for a qualitative understanding of the electronic structure. Indeed, for the AGNR with $\mathrm{mod}(N+1,3) = 0$ the sheets are divided into a multiple of three equally wide sections. Hence, the $k_y = 2/3k_{\max}$ line goes though the K point (fourth sheet; Fig. 3) predicting a ribbon with an anomalously small bandgap.[30] After applying the selection

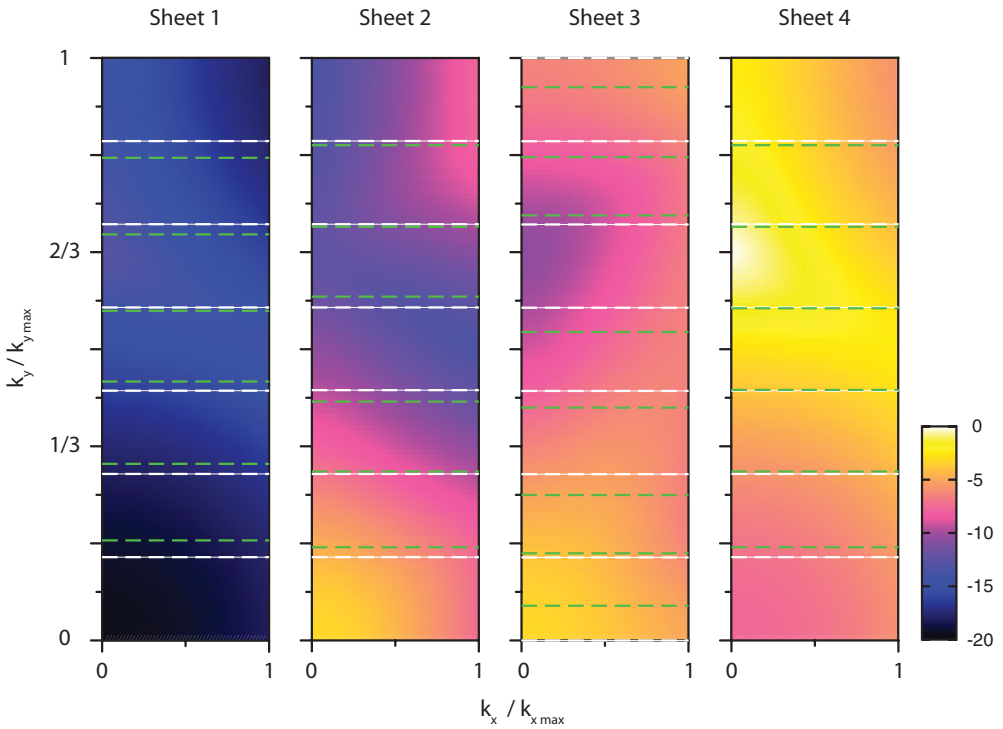

FIG. 3. (Color online) Energy bands for the $N = 6$ AGNR [long-dashed (green) lines] plotted on the graphene dispersion sheets in the $\mathbf{k}_x$, $\mathbf{k}_y$ plane. Dashed (white) lines indicate estimates based on the selection rule; see Eq. (1).

rule to the other ribbons as well, we recover the values for the band gaps obtained by earlier tight-binding calculations, with nearest-neighbor hopping.[30,43,44] In addition, the selection also works for all the other sheets. The particularities of these sheets is encoded not only in the K-point behavior but also in the position of Van Hove singularities. Since the positioning of the electronic levels with respect to these features also oscillates with period 3, one expects that the oscillation behavior of the electronic structure also carries over to the atomic geometry.

IV. ATOMIC STRUCTURE OF AN H-TERMINATED AGNR

We now investigate how the electronic structure translates into the atomistics of the AGNR, which we have also determined within our *ab initio* approach. For the cell geometry we adopt the nomenclature depicted in Fig. 1. The extension

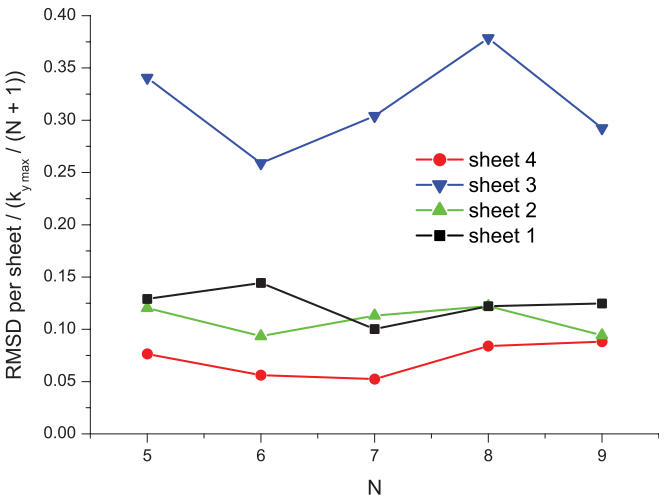

FIG. 4. (Color online) Root mean square deviation per sheet of the fitted k_y values to the values predicted by the selection rule. The deviations in sheets 1, 2, and 4 remain smaller than 15% of the line spacings independent of the ribbon width N. The bigger deviations in the fourth sheet result from the presence of the hydrogen edge.

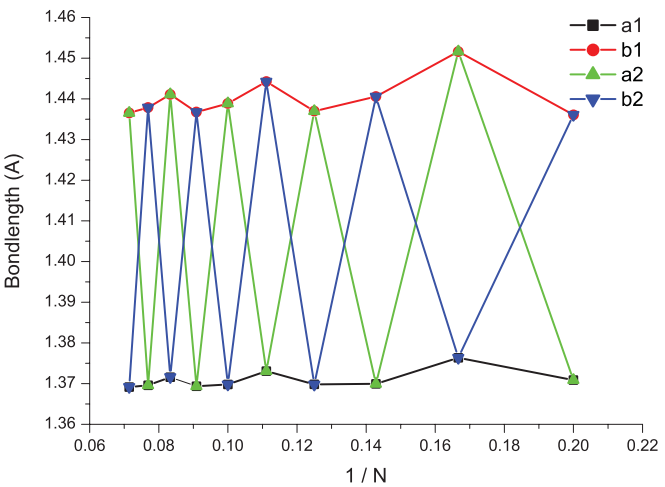

FIG. 5. (Color online) Evolution of the edge C-C bonds plotted against $1/N$. For the location of the bonds, a1, a2, b1, and b2, see Fig. 1. The growth of the sample width is in the negative y direction, so a2 and b2 oscillate, while a1 and b1 do not. The lower trace corresponds to the outer bonds; the upper trace, to the (more) inner bonds.

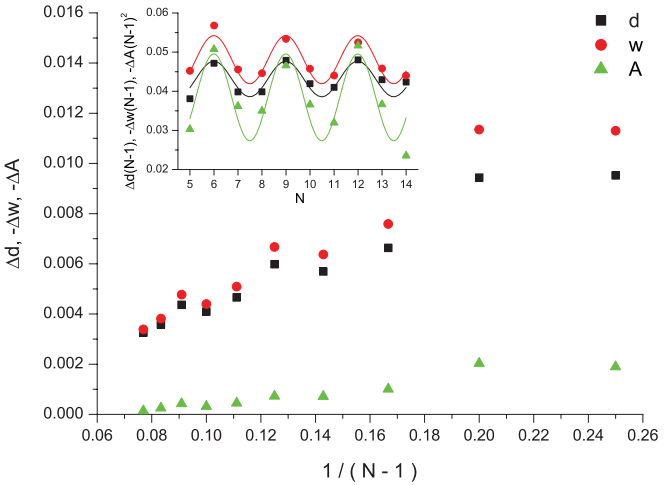

FIG. 6. (Color online) Relative deformation of the geometry of the unit cell for hydrogen-terminated graphene armchair nanoribbons as a function of the inverse of the width $\frac{1}{N-1}$; values for $N = 5 \ldots 14$ have been considered. Insets highlight the corresponding power-law dependencies on the ribbon width, which has the remarkable feature that the oscillations do not experience significant damping.

of the unit cell in the x and y directions is indicated by d and w, respectively. For ease of comparison to bulk values we introduce the dimensionless quantities $\Delta d = \frac{d}{\sqrt{3}a_0} - 1, \Delta w = \frac{w}{(N-1)(a_0/2)} - 1$, and $\Delta A = (\Delta d + 1)(\Delta w + 1) - 1$, with a_0 the lattice parameter of bulk graphene calculated using the same functional and accuracy. All three become 0 in the bulk limit, $N \to \infty$.

In a monohydrogen-terminated AGNR (H-AGNR), each carbon edge atom binds two other carbon atoms and one hydrogen atom. Considering the atomic structure of H-AGNRs, this leads to a twofold periodicity associated with N even and N odd (see Fig. 1). AGNRs of consecutive widths, $N = 2n$ and $N = 2n + 1$, have different structural patterns; $2n$ AGNRs exhibit $n - 1$ hexagons in all lateral sections, while $(2n + 1)$ AGNRs have a series of alternating n and $n - 1$ hexagons. The effect of this pattern can be visualized by plotting the edge C–C bond lengths for the fully relaxed structures over the reciprocal of the ribbon width $1/N$ (Fig. 5).

The way the edge exerts a pressure on the ribbon is, however, nontrivial. Although the overall effect is elongating, we observe that the outer C–C bonds a1 are always shorter than the inner ones b1 (Fig. 1). Even more, the sum of a1 and a2 is less than 2 times the optimal bulk C–C. The difference survives in the large-N limit. The main cause of the elongation is hence not a change in bond lengths but the opening of the angles α and β.

The effect is also displayed in Fig. 6, which now emphasizes healing of the geometry of the unit cell and allows for a simplified quantitative analysis:

$$\Delta d = \kappa_d(N)/(N - 1).$$

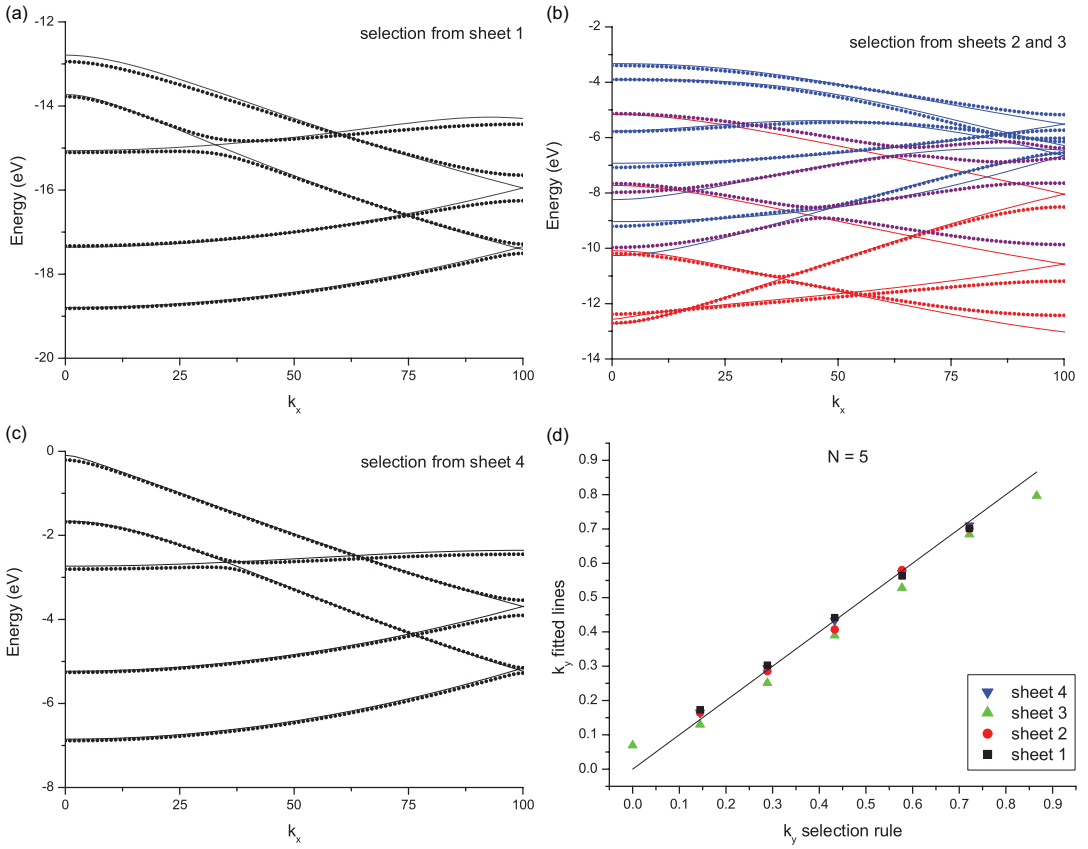

FIG. 7. (Color online) (a–c) Comparison of the calculated band structure (dots) of the $N = 5$ AGNR to the fitted band structure obtained by selecting curves at fixed k_y values from the graphene dispersion sheets (lines). Red lines in (b) belong to sheet 2; blue lines, to sheet 3. (d) Comparison of the fitted k_y values to the k_y values obtained from the selection rule given by Eq. (1).

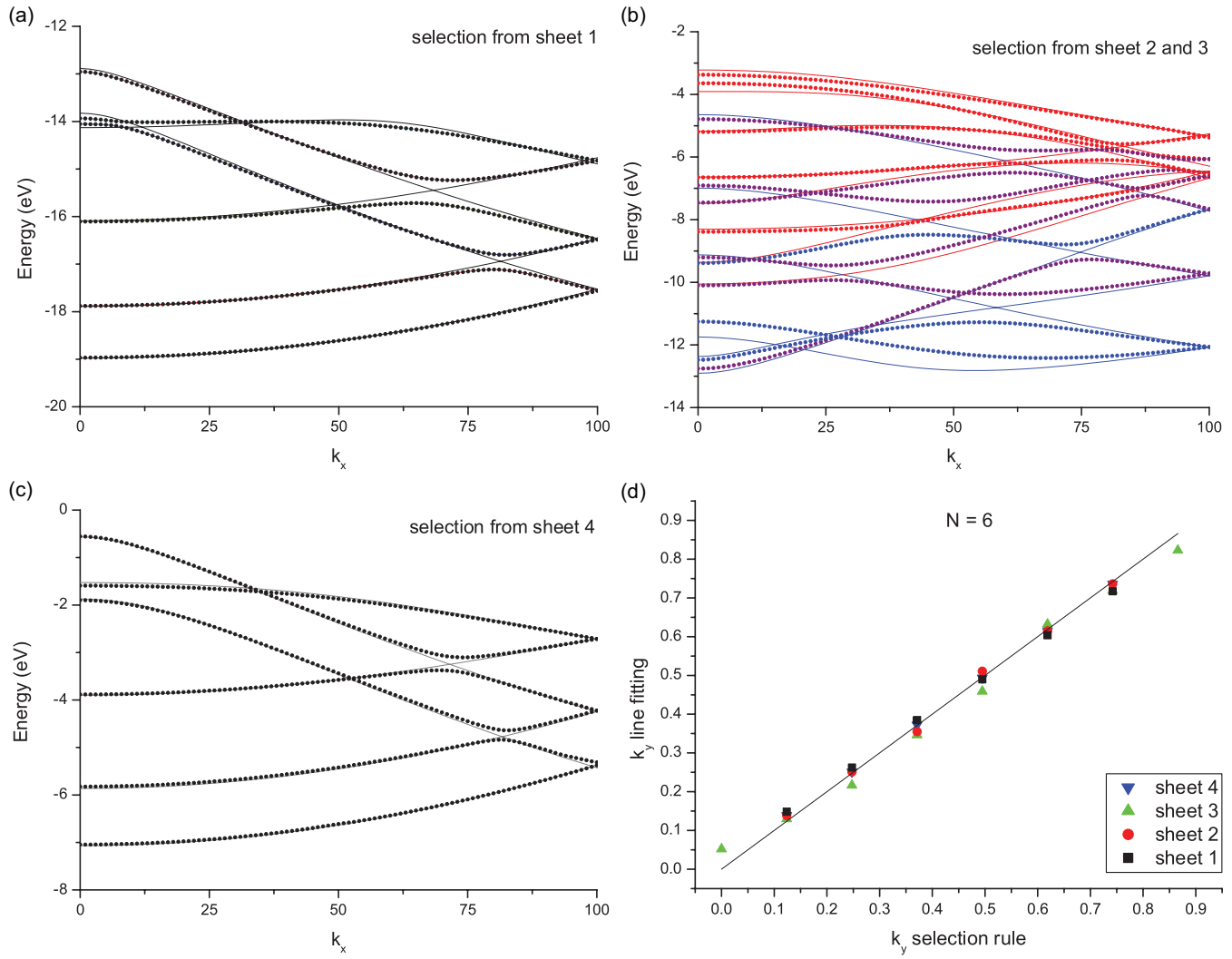

FIG. 8. (Color online) The same comparison as in Fig. 7, for an $N = 6$ ribbon.

The prefactor is found to match the empirical form,

$$\kappa_d(N) \sim \kappa_d^{(0)}\left(1 + \kappa_d^{(1)} \cos\left(2\pi N/3\right)\right), \tag{2}$$

with fitting parameters $\kappa_d^{(0)} \approx 0.04$ and $\kappa_d^{(1)} \approx 0.11$, see the inset of Fig. 6: it carries information about the strength of the edge-induced force per length, i.e., the chemical edge termination, and the elastic response of the AGNR, which again incorporates the effective boundary conditions imposed on the ribbon's wave functions.

A striking aspect of Figs. 5 and 6 is the pronounced oscillation in N with period 3. It translates into the $\cos(2\pi N/3)$ term in Eq. (2), which we take as evidence of the boundary conditions feeding back into the ribbon's elasticity. By contrast, the twofold periodicity originating from even or odd N is largely suppressed. This suppression is understood in the following way. As long as bond stretching is not too strong, we reside in the regime of linear elasticity. Then there is, by definition, no cross-talk between the stimulating stretching forces from either edge; the ribbon's response is essentially a superposition of two independent stimuli, one from each edge, each one being largely insensitive to details of termination of the other edge. Hence, the twofold periodicity is suppressed.[45]

A simple argument how the period 3 oscillations of the electronic structure translate into the atomic structure relies on the observation that the Brillouin zone has its most important structural elements at the points of higher symmetry: Γ, K, and M points (cf. Figs. 1 and 2). They are situated at $k_y/k_{\max} = 0$, $1/2$, $2/3$, 1. We have already seen from the selection rule that there is a level very close to the K point whenever $(N + 1)/3$ is an integer. Now quite generally the electronic structure determines the electronic ground-state energy, which in turn is closely intertwined with the lattice geometry: both follow from the same energy optimization routine. Therefore, it is hardly surprising that repetitive patterns (with N) of one of them also translate into the other. Here, the repetitive pattern appears in the structure of all electronic bands. Because this is true for all bands including binding ones, the feedback into the atomic structure is sizable.

It is a remarkable feature of Eq. (2) that the oscillations do not experience significant damping (at least within the

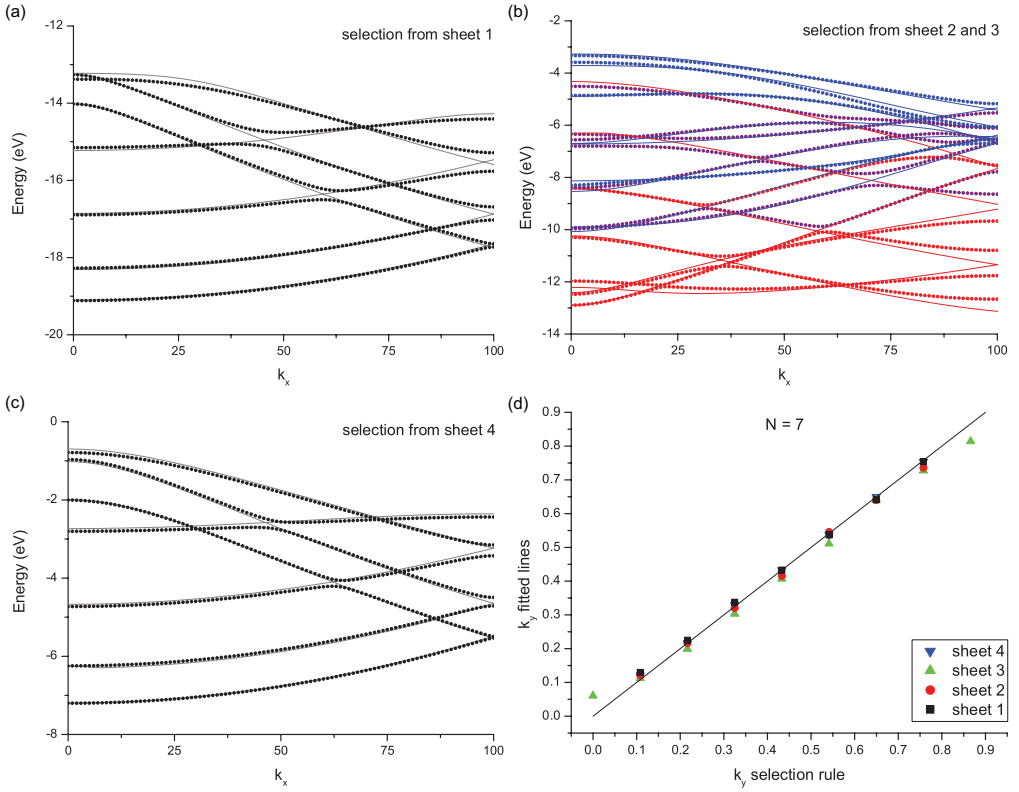

FIG. 9. (Color online) The same comparison as in Fig. 7, for an $N = 7$ ribbon.

system sizes available to our numerics). In the absence of perturbations not included in our model such as ripples and other inhomogeneities, we expect that this statement should remain valid as long as the deviation between the true position of the AGNR band and the prediction based on the selection rules, Eq. (1), remains small compared to Δk_y. Judging from

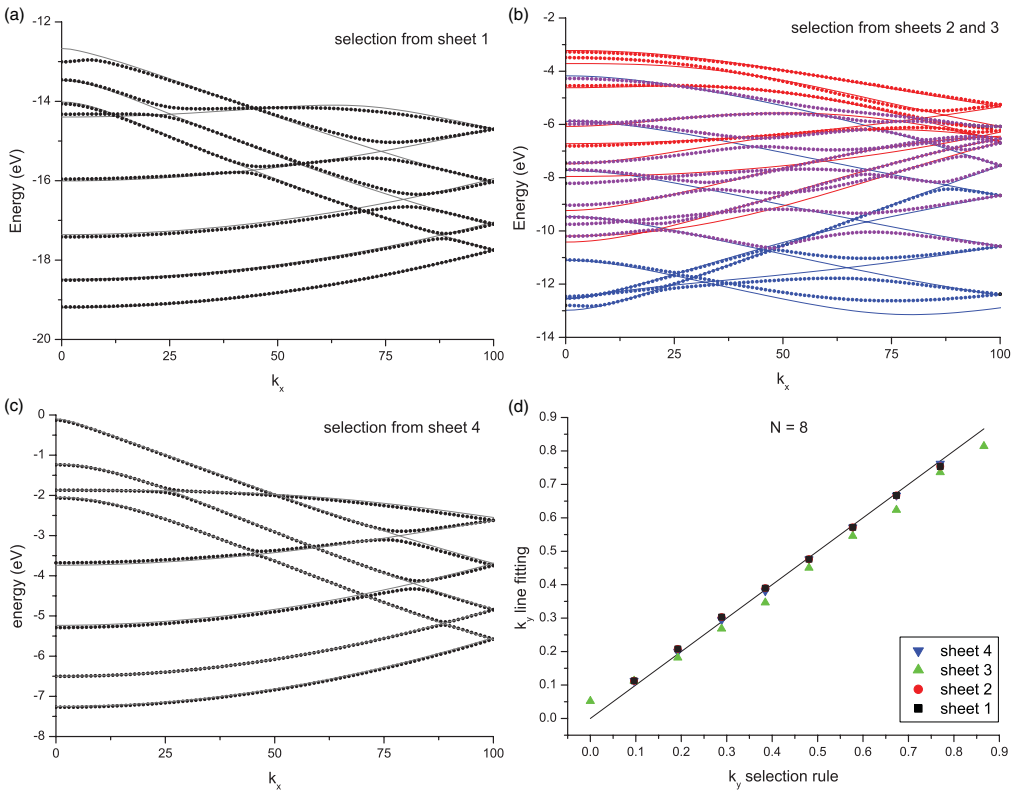

FIG. 10. (Color online) The same comparison as in Fig. 7, for an $N = 8$ ribbon.

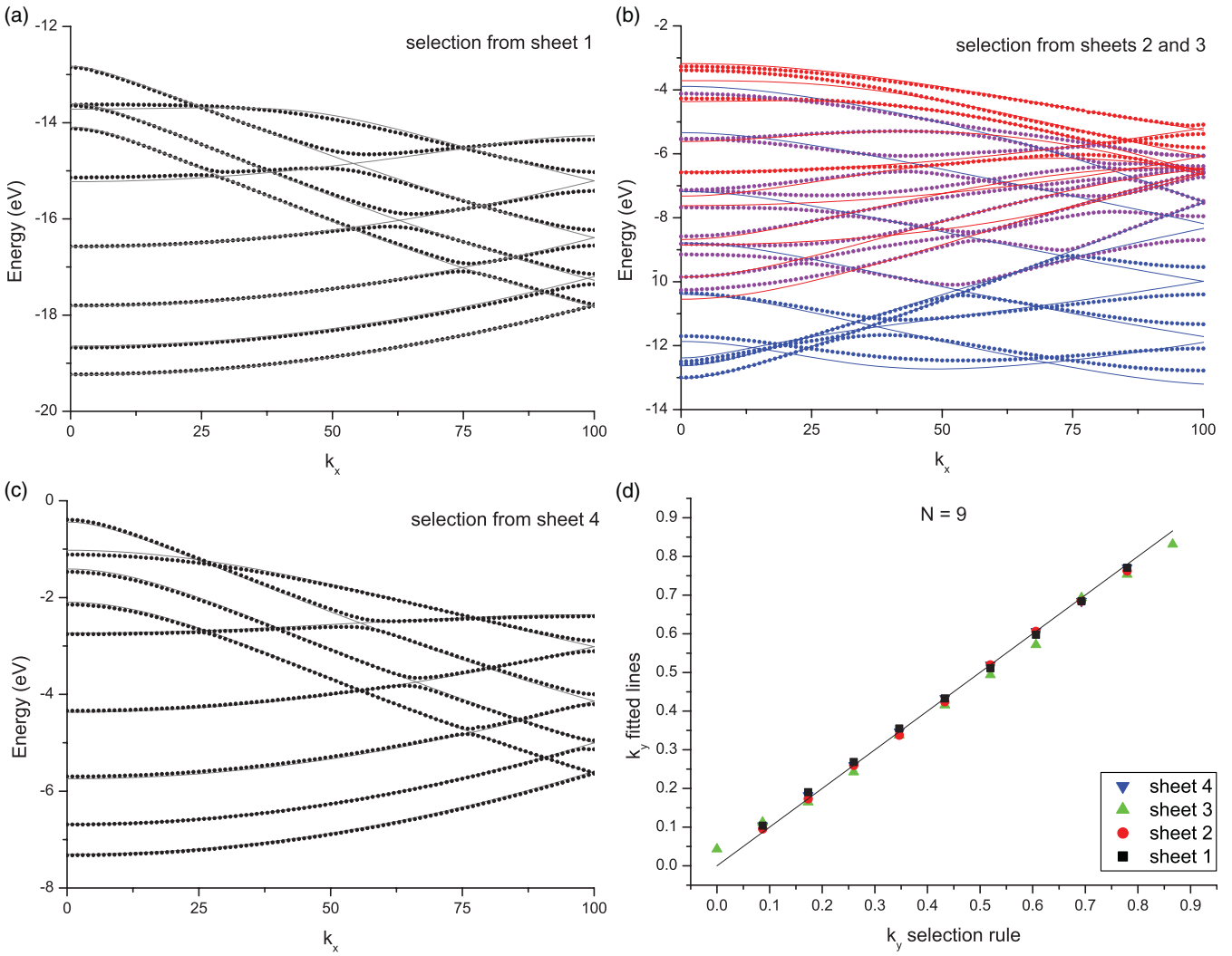

FIG. 11. (Color online) The same comparison as in Fig. 7, for an $N = 9$ ribbon.

Fig. 4, this could be true at least into the regime where the aspect ratio N/L is still low.

Elastic material responses are usually (approximately) volume conserving. It is therefore reassuring to see that this is also the case in the present situation. Stretching the ribbon in the longitudinal direction evokes a transverse contraction (see Fig. 6) which eliminates, in the leading order, the strain effect on the volume of the unit cell,

$$\Delta A = \frac{\kappa_A(N)}{(N-1)^2}, \tag{3}$$

where $\kappa_A(N)$ is of the form of (2) with constants $\kappa_A^{(0)} \approx 0.04$ and $\kappa_A^{(1)} \approx 0.2$, see the inset of Fig. 6.

V. CONCLUSIONS

We have studied quantum size effects in AGNRs with hydrogen termination using DFT in the Kohn-Sham formulation. By formulating "selection rules" that allow us to extract (approximately) the electronic structure of the AGNR bands starting from the four graphene dispersion sheets, we have predicted a threefold periodicity of the ribbon's electronic structure in the ribbon width N, which was confirmed by *ab initio* results. We have also observed how this threefold electronic periodicity carries over into the atomic structure of AGNRs.

Our results imply that quantum size effects can be studied experimentally in H-AGNRs by atomic structure determination, namely, by comparing the length per carbon slice of AGNRs of neighboring widths $N, N+1, \ldots$. This is in marked contrast to traditional approaches in meso- and nanoscopic structures, which investigate quantum size effects near the bandgap by directly probing the electronic excitation spectrum, e.g., in transport measurements. At a length of about 1850 carbon slices, an $N = 12$ ribbon will be a full chain of carbon atoms longer than an $N = 11$ ribbon with the same number of chains, whereas an $N = 13$ ribbon will be the same amount shorter. This difference is large enough that it could be detected experimentally. We expect that a termination other than hydrogen will change only the amount of edge-induced stress, and not the mechanism underlying the elastic response. Hence, the values of the constants κ will change, but not the oscillating behavior.

ACKNOWLEDGMENTS

Financial support from the Center for Functional Nanostructures and cpu time allocation at the OPUS[IB] and hc3

clusters at the Karlsruhe Institute of Technology, Steinbuch Center for Computing, are gratefully acknowledged.

APPENDIX: COMPARISON OF THE REAL BAND STRUCTURE TO THE SELECTION RULE

As described in Sec. III, for each dispersion sheet of bulk graphene (see Fig. 3), a set of k_y values in the Brioullin zone (see Fig. 1) was fitted such that the obtained set of $\epsilon_{k_y}(k_x)$ functions most closely resembles the band structure of the AGNR in question. This procedure was performed for AGNRs with $N = 5$ to 9. Figures 7(a)–7(c) to 11(a)–11(c) show a comparison of these functions to the actual calculated ribbon dispersion bands. Figures 7(d) to 11(d) compare these fitted k_y values to the values obtained from the selection rule expressed in Eq. (1).

*Present address: Institut Néel, CNRS, 25 Avenue des Martyrs, B.P. 166, F-38042 Grenoble, France.
†michiel.setten@kit.edu

[1] K. Novoselov, A. Geim, S. Morozov, D. Jiang, M. Katsnelson, I. Grigorieva, S. Dubonos, and A. Firsov, Nature **438**, 197 (2005).
[2] A. H. Castro Neto, F. Guinea, N. M. R. Peres, K. S. Novoselov, and A. K. Geim, Rev. Mod. Phys. **81**, 109 (2009).
[3] A. K. Geim and K. S. Novoselov, Nat. Mater. **6**, 183 (2007) .
[4] M. Y. Han, B. Ozyilmaz, Y. Zhang, and P. Kim, Phys. Rev. Lett. **98**, 206805 (2007).
[5] K. Wakabayashi, M. Fujita, H. Ajiki, and M. Sigrist, Phys. Rev. B **59**, 8271 (1999) .
[6] K. A. Ritter and J. W. Lyding, Nat. Mater. **8**, 235 (2009).
[7] L. Jiao, L. Zhang, X. Wang, G. Diankov, and H. Dai, Nature **458**, 877 (2009).
[8] L. Doessel, L. Gherghel, X. Feng, and K. Muellen, Angew. Chem. Int. Ed. **50**, 2540 (2011).
[9] X. Jia, J. Campos-Delgado, M. Terrones, V. Meunier, and M. S. Dresselhaus, Nanoscale **3**, 86 (2011).
[10] S. M. M. Dubois, Z. Zanolli, X. Declerck, and J. C. Charlier, Eur. Phys. J. B **72**, 1 (2009).
[11] T. Wassmann, A. P. Seitsonen, A. M. Saitta, M. Lazzeri, and F. Mauri, Phys. Status Solidi B Basic Solid State Phys. **246**, 2586 (2009).
[12] D. V. Kosynkin, A. L. Higginbotham, A. Sinitskii, J. R. Lomeda, A. Dimiev, B. K. Price, and J. M. Tour, Nature **458**, 872 (2009).
[13] X. Wang and H. Dai, Nat. Chem. **2**, 661 (2010).
[14] J. Cai, P. Ruffieux, R. Jaafar, M. Bieri, T. Braun, S. Blankenburg, M. Muoth, A. P. Seitsonen, M. Saleh, X. Feng, K. Muellen, and R. Fasel, Nature **466**, 470 (2010).
[15] D. Gosalbez-Martinez, J. J. Palacios, and J. Fernandez-Rossier, Phys. Rev. B **83**, 115436 (2011) .
[16] M. Vanin, J. Gath, K. S. Thygesen, and K. W. Jacobsen, Phys. Rev. B **82**, 195411 (2010) .
[17] L. Yang, J. Xiaowei, L. Zhongfan, and l. Zhirong, Nano. Res. **3**, 545 (2010) .
[18] S. K. Hämäläinen, Z. Sun, M. P. Boneschanscher, A. Uppstu, M. Ijäs, A. Harju, D. Vanmaekelbergh, and P. Liljeroth, Phys. Rev. Lett. **107**, 236803 (2011).
[19] S. Bera, A. Arnold, F. Evers, R. Narayanan, and P. Wolfle, Phys. Rev. B **82**, 195445 (2010).
[20] M. Zarea and N. Sandler, New J. Phys. **11**, 095014 (2009).
[21] T. Wassmann, A. P. Seitsonen, A. M. Saitta, M. Lazzeri, and F. Mauri, Phys. Rev. Lett. **101**, 096402 (2008).
[22] J. J. Palacios, J. Fernandez-Rossier, L. Brey, and H. A. Fertig, Semicond. Sci. Technol. **25**, 033003 (2010) .
[23] X. Blase, C. Adessi, B. Biel, A. Lopez-Bezanilla, M. V. Fernandez-Serra, E. R. Margine, F. Triozon, and S. Roche, Phys. Status Solidi B Basic Solid State Phys. **247**, 2962 (2010).
[24] S. S. Yu, Q. B. Wen, W. T. Zheng, and Q. Jiang, Mol. Simul. **34**, 1085 (2008).
[25] L. Pisani, J. A. Chan, B. Montanari, and N. M. Harrison, Phys. Rev. B **75**, 064418 (2007).
[26] V. Barone, O. Hod, and G. E. Scuseria, Nano Lett. **6**, 2748 (2006).
[27] A. V. Rozhkov, S. Savel'ev, and F. Nori, Phys. Rev. B **79**, 125420 (2009).
[28] D. Gunlycke and C. T. White, Phys. Rev. B **77**, 115116 (2008).
[29] L. Yang, C.-H. Park, Y.-W. Son, M. L. Cohen, and S. G. Louie, Phys. Rev. Lett. **99**, 186801 (2007).
[30] Y.-W. Son, M. L. Cohen, and S. G. Louie, Phys. Rev. Lett. **97**, 216803 (2006).
[31] Z. Chen, Y.-M. Lin, M. J. Rooks, and P. Avouris, Physica E **40**(2), 228 (2007) .
[32] B. Huang, M. Liu, N. Su, J. Wu, W. Duan, B.-l. Gu, and F. Liu, Phys. Rev. Lett. **102**, 166404 (2009) .
[33] G. Kresse and D. Joubert, Phys. Rev. B **59**, 1758 (1999) .
[34] P. E. Blöchl, Phys. Rev. B **50**, 17953 (1994) .
[35] G. Kresse and J. Furthmüller, Phys. Rev. B **54**, 11169 (1996) .
[36] G. Kresse and J. Furthmüller, Comput. Mater. Sci. **6**, 15 (1996) .
[37] J. Hafner, J. Comput. Chem. **29**, 2044 (2008) .
[38] J. P. Perdew, J. A. Chevary, S. H. Vosko, K. A. Jackson, M. R. Pederson, D. J. Singh, and C. Fiolhais, Phys. Rev. B **46**, 6671 (1992) .
[39] R. C. Weast and M. J. Astle, *CRC Handbook of Chemistry and Physics*, 89th ed. (CRC Press, New York, 2009) .
[40] Often, computational studies of graphene apply LDA. The motivation is that the interaction between graphene sheets is described better by the LDA than by the GGA; in most GGAs the layers forming graphite do not even bond .
[41] G. G. Samsonidze, R. Saito, N. Kobayashi, A. Gruneis, J. Jiang, A. Jorio, S. G. Chou, G. Dresselhaus, and M. S. Dresselhaus, Appl. Phys. Lett. **85**, 5703 (2004) .
[42] L. Brey and H. A. Fertig, Phys. Rev. B **73**, 235411 (2006) .
[43] Z. F. Wang, Q. Li, H. Zheng, H. Ren, H. Su, Q. W. Shi, and J. Chen, Phys. Rev. B **75**, 113406 (2007).
[44] X. W. Zhang and G. W. Yang, J. Phys. Chem. C **113**, 4662 (2009).
[45] The most important contribution to the binding of sp_2-hybridized carbon atoms is made by in-plane σ bonds. Stretching at one edge of the AGNR faces a restoring force that originates from the inner σ bonds. Most of this restoring force comes from the innermost carbon atoms; only a small contribution is made by atoms of the opposing edge. For this reason, the elastic deformation of the carbon lattice responding to the H_2-induced stretch on one edge is hardly sensitive to the termination of the other edge.